

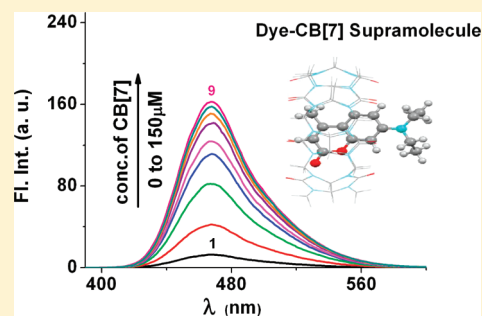
Supramolecular Interaction of Coumarin 1 Dye with Cucurbit[7]uril as Host: Combined Experimental and Theoretical Study

Monika Gupta,[†] Dilip K. Maity,^{*,‡} Manoj K. Singh,[§] Sandip K. Nayak,^{||} and Alok K. Ray^{*,†}

[†]Laser & Plasma Technology Division, [‡]Theoretical Chemistry Section, [§]Atomic & Molecular Physics Division, and ^{||}Bio-organic Division, Bhabha Atomic Research Centre, Mumbai-400 085, India

S Supporting Information

ABSTRACT: Molecules of the coumarin family have fluorescence characteristics that are highly sensitive to their environment, and thus, they have been used as fluorescent sensors in chemical and biological systems. However, the very poor fluorescence yield of most coumarin dyes in aqueous media limits their applications. We have adopted a supramolecular strategy to improve the fluorescence intensity of coumarin dye through its interaction with the relatively new host cucurbit[7]uril (CB[7]). The virtually nonfluorescent coumarin 1 ($\Phi_f = 0.04$) was converted into a highly fluorescent ($\Phi_f = 0.52$) entity in water upon addition of the nonfluorescent host CB[7]. Various spectroscopy techniques, namely, UV–vis absorption and steady-state and time-resolved fluorescence spectroscopies, established the formation of a strong 1:1 dye–CB[7] inclusion complex with a high binding constant of $(1.2 \pm 0.1) \times 10^5 \text{ M}^{-1}$ for the dye. The stable inclusion complex of the neutral molecule was supported by density-functional-theory- (DFT-) based quantum chemical calculations. Energy decomposition analysis of various interaction factors in the host–guest complex revealed that key components providing stability to the complex were electrostatic, polarization, and charge-transfer energies. These new results on the formation of a strong inclusion complex of the versatile fluorophore coumarin 1 with the nontoxic host CB[7] could lead to the design of efficient molecular-scale biological probes, sensors, and photostable aqueous UV dye lasers.



1. INTRODUCTION

Noncovalent supramolecular interactions are omnipresent in nature. The fundamental study of these noncovalent interactions has occupied the forefront of contemporary research as they have been judiciously used in a wide range of applications including the development of catalysts, stationary phases in chromatographic separations, sequestration of different metal ions from solutions, chemical sensors, self-assembly of nanomaterials, and drug development.^{1–4} All of these applications require the availability of receptors, natural or non-natural oligomers and polymers or solid-state hosts, that interact with their guests with high affinity through highly selective binding processes. In response, supramolecular chemists have designed, synthesized, and evaluated the recognition properties of a wide variety of non-natural receptors, including cyclodextrins, crown ethers, calixarenes, and cyclophanes, that display exceptional affinities and selectivities.⁵

Of late, members of a new class of supramolecular hosts called cucurbit[n]urils (CB[n]), which are composed of glycoluril units linked by a pair of methylene groups and have fairly rigid hydrophobic cavities of low polarizability, have been synthesized.⁶ They have been used as efficient hosts⁷ that can be accessed through their carbonyl-lined portals. The cavity sizes of CB[n] hosts and their derivatives exceed the range available with the widely studied α -, β -, and γ -cyclodextrins. Among the CB[n] family, cucurbit[7]uril (CB[7]) has

substantially higher water solubility than CB[6] and CB[8], as well as a more voluminous cavity than its water-soluble analogue CB[5], and can thus bind a wider range of guests in aqueous solutions. In addition to the usual hydrophobic effect in water, which favors inclusion of organic guests within the CB[7] cavity, CB[7] provides another distinct supramolecular interaction, namely, ion–dipole interactions at carbonyl-lined portals, that promotes the binding of the cationic sites of organic guests. Recently, the CB[7] host was used to form strong and stable inclusion complexes with some fluorescent dyes^{8–10} to improve their fluorescence yields and photochemical stabilities in water, which also led to other novel applications such as operation of efficient and photostable aqueous dye lasers.¹¹ Moreover, the low toxicity of CBs,¹² including a high cell tolerance in living biological systems at a concentration of up to 1 mM, has been demonstrated, indicating their potential use as molecular containers in advanced drug-delivery systems.

Coumarins are a versatile class of hydrophobic organic fluorophores¹³ found in many plants and medicines that are used in fluorescence microscopy as sensitive fluorescent probes for proteins and other biological molecules, in dye-sensitized solar cells, and in dye lasers as UV dyes, among other

Received: February 8, 2012

Revised: April 11, 2012

Published: April 13, 2012

applications. However, the preferred use of aqueous solutions of coumarin dyes for these applications has been limited because of low solubility, dramatic reductions in fluorescence intensity, and photochemical instability in water. These problems can be largely overcome by complex formation with the host CB[7].¹⁴

For a preliminary study on the interaction of CB[7] with coumarin, 7-diethylamino-4-methylcoumarin, or coumarin 1, a widely used fluorescent molecule in organic solvents that is virtually nonfluorescent in water, was used as a guest. In coumarin 1 dye, the 7-diethylamine moiety can play an important role in modulating the molecule's photophysics in aqueous solutions. Earlier, Nau and Mohanty^{14c} reported that the fluorescence intensity of aqueous solutions of coumarin 102 dye is enhanced in the presence of the host CB[7], but by only a factor of 1.14. A recent report^{14a} on the inclusion behavior of parent coumarin dye with CB[7] as a biological fluorescence probe in aqueous solutions inspired us to carry out a detailed study on the interaction of coumarin 1 with CB[7]. To the best of our knowledge, the supramolecular interaction of the host CB[7] with amino-substituted coumarin derivatives has not yet been studied.

In this article, we present our results on the effective inclusion of coumarin 1 dye inside the cavity of nonfluorescent host CB[7], thereby significantly improving the dye's fluorescence intensity (~ 13 -fold) in aqueous systems. The beneficial effects on the photophysical properties of coumarin 1 dye in water upon addition of CB[7] were investigated systematically by various spectroscopy techniques including UV-vis absorption and steady-state and time-resolved fluorescence spectroscopies. For comparison, the photophysical properties of the dye in ethanol were also studied. The high interaction energy and stable inclusion geometry of coumarin 1 dye were confirmed by density functional theory (DFT) based all-electron calculations. Moreover, energy decomposition analysis was performed to identify and quantify the types of interactions in the host-guest complex. These results could lead to some promising applications of aqueous solutions of the dye as a sensitive and efficient fluorescent probe in chemical and biological research and in the area of UV dye lasers. The chemical structures of the coumarin 1 and CB[7] molecules are displayed in Figure 1.

2. EXPERIMENTAL SECTION

Laser-grade coumarin 1 (7-diethylamino-4-methylcoumarin) and coumarin 2 (4,6-dimethyl-7-ethylaminocoumarin) dyes

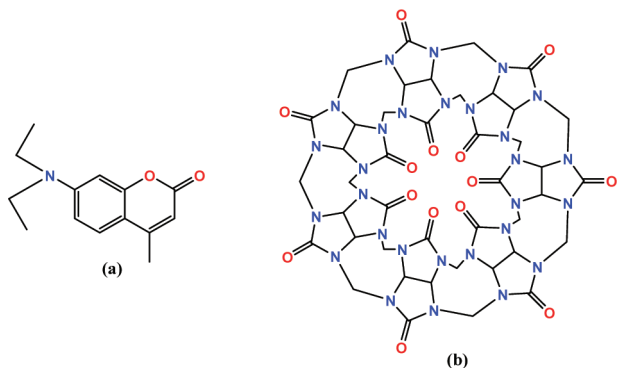


Figure 1. Molecular structures of (a) coumarin 1 and (b) cucurbit[7]uril (CB[7]).

were obtained from Lambda Physik (Göttingen, Germany); their purity was checked by thin-layer chromatography (TLC) and ¹H nuclear magnetic resonance (NMR) spectroscopy in CDCl₃, and they were used without further purification. The host cucurbit[7]uril was synthesized, separated, and purified following procedures reported by Kim et al. and Day et al.,^{6b,c} and its purity was verified by ¹H and ¹³C NMR spectroscopies and electrospray ionization mass spectrometry (ESI-MS). Spectroscopy-grade ethyl alcohol and nanopure water, obtained by passing distilled water through a Thermo-Scientific Nanopure water system, were used for all dye-solution preparations.

Absorption and steady-state fluorescence spectra of dye solutions (5–20 μ M) were obtained using a commercial UV-vis spectrophotometer (JASCO V-550) and spectrofluorimeter (JASCO FP-6500), respectively. Time-resolved fluorescence measurements for fluorescence lifetimes and rotational orientation times of the dye and its supramolecular complex were carried out using a time-correlated single-photon-counting (TCSPC) setup (FluoTime-200 from PicoQuant GmbH, Berlin, Germany). Coumarin 1 dye was found to be highly soluble in ethanol, but its solubility was very low (< 60 μ M) in aqueous media. An ethanol solution of coumarin 2 dye was used as a fluorescence standard for estimating the fluorescence yield of the coumarin 1 dye–CB[7] system.

3. RESULTS AND DISCUSSION

3.1. Absorption Studies. A bathochromic shift was observed in absorption spectra of coumarin 1 dye in water. The longest-wavelength absorption maxima (λ_{max}^a) of the dye in ethanol and water were at 373 and 380 nm, respectively. This solvatochromic effect due to the higher polarity of water agrees with the reported data.¹⁵ However, addition of the host CB[7] to aqueous solutions of the dye induced progressively red-shifted absorption spectra. The maximum shift in the λ_{max}^a value of the dye (~ 7.2 μ M) was to 396 nm, at a CB[7] concentration of ~ 150 μ M, 20 times the typical dye concentration (Figure 2).

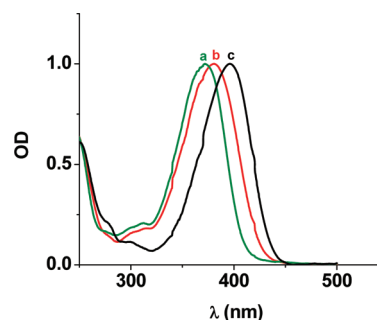


Figure 2. Comparative absorption spectra of coumarin 1 dye in (a) ethanol, (b) water, and (c) water with a high concentration of CB[7]. The spectra were normalized to clearly differentiate the relative shifts in absorption maximum.

The observation of a red shift of the absorption maximum of the dye upon addition of the host CB[7], despite its low-polarity cavity, indicates the influence of other factors on the absorption spectrum such as rearrangement of the hydrogen bonds between the dye and water molecules. The modulation of the absorption spectrum of the dye in the presence of CB[7] points toward their interaction.

3.2. Steady-State Fluorescence Studies. The fluorescence spectrum of the dye was also more red-shifted in polar

water ($\lambda_{\text{max}}^f \approx 468$ nm) than in ethanol ($\lambda_{\text{max}}^f \approx 448$ nm). A larger solvatochromic shift (20 nm) was found in the emission spectrum than in the absorption spectrum (7 nm) of the dye when changing from ethanol to water. This behavior could be correlated with a significantly higher dipole moment of the excited state (S_1) in comparison to the ground state (S_0) of the dye molecule, which also induces a large Stoke's shift of the dye upon electronic excitation. In analogy with its close analogue C311 (7-dimethylamino-4-methylcoumarin), the dipole moment (μ) of the coumarin 1 molecule could increase¹⁶ from 6.0 D (at S_0) to 7.3 D (at S_1). Therefore, the dye molecule in the excited state would undergo a higher energy stabilization mediated by stronger geometrical and solvent relaxation in the polar and protic water. Hence, the photophysics of coumarin 1 indicates that its ground and excited electronic states behave quite differently.

In contrast to the red-shifted absorption spectra of aqueous solutions of the dye in the presence of the CB[7], the emission maximum (λ_{max}^f) showed a negligible shift (Figure 3). The

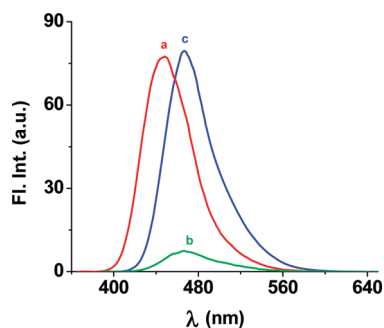


Figure 3. Comparative fluorescence spectra of coumarin 1 dye in (a) ethanol, (b) water, and (c) water with a high concentration of CB[7]. The excitation wavelength was 385 nm.

cavity of CB[7] is known^{8b,17} to have a high hydrophobicity and a very low polarizability and polarity. The arrangement of hydrogen bonding^{15b,16} between water and the amine nitrogen, carbonyl oxygen, and alkyl groups of the coumarin 1 molecule would change significantly upon the interaction of the coumarin 1 molecule with the cavity of CB[7]. The interplay of these interactions might be responsible for the observation (Table 1) of a bathochromic shift in the absorption spectrum but no change in emission transition energy of the dye in water upon addition of the host CB[7].

As expected, the fluorescence intensity of the dye was found to decrease dramatically in water in comparison to that in ethanol, which has been explained as resulting from the formation of a twisted intramolecular charge-transfer (TICT) state of the coumarin 1 molecule in polar and protic water. However, the fluorescence intensity was observed to increase strongly in the presence of even a small amount of CB[7] in water and to attain a peak intensity value similar to that in ethanol at a high concentration (~ 150 μM) of CB[7] relative to that of the dye (~ 7.2 μM). A large increase (~ 13 -fold) in

the fluorescence intensity of the dye in water upon addition of the host CB[7] (Figure 4) points toward strong binding

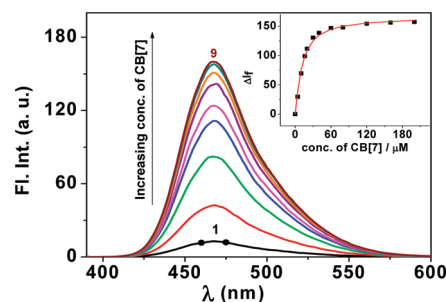


Figure 4. Steady-state fluorescence spectra of coumarin 1 dye (7.2 μM) with increasing concentration of CB[7]: (1) 0, (2) 4, (3) 16, (4) 30, (5) 40, (6) 60, (7) 80, (8) 120, and (9) 150 μM . Inset: Dependence of the increase in the fluorescence intensity (ΔI_f) of the dye on the addition of CB[7] in aqueous solution. The solid line represents the best fit of the data corresponding to a 1:1 inclusion complex, indicating a binding constant of $K = 1.2 \times 10^5 \text{ M}^{-1}$.

between the dye and the host. Interestingly, the fluorescence quantum yield (Φ_f) of the dye in water in the presence of a high concentration of CB[7] was found (see the Supporting Information) to have a value similar to that in ethanol ($\Phi_f \approx 0.54$).

A systematic improvement in the fluorescence intensity of the dye in water with a progressive addition of the host CB[7] can be linked to the confinement of the guest within the cavity of CB[7], concurrent with the dominance of hydrophobic effects related to the removal of high-energy water molecules¹⁷ from the cavity of CB[7]. To confirm the stoichiometry of the dye–CB[7] complex, the peak fluorescence intensities of aqueous solutions of the dye were measured at varying mole-fraction concentrations of CB[7] at a constant total concentration of dye and CB[7]. The peak emission intensity values of these dye–CB[7] solutions were correlated by a continuous variation method of Job's plot (Figure S3 in the Supporting Information), which showed a maximum at a value of 0.5 for the mole fraction of CB[7], indicating a 1:1 binding stoichiometry.

The binding constant of the dye with CB[7] was determined by a nonlinear fitting of the observed increase in fluorescence intensity (ΔI_f) as a function of CB[7] concentration using a 1:1 complex formation equation¹⁸

$$\Delta I_f = I_{\text{obs}} - I_{\text{dye}}^0 \quad (1)$$

or

$$\Delta I_f = \left(1 - \frac{[\text{dye}]_{\text{eq}}}{[\text{dye}]_0} \right) (I_{\text{dye,CB[7]}}^{\infty} - I_{\text{dye}}^0) \quad (2)$$

where $[\text{dye}]_0$ and $[\text{dye}]_{\text{eq}}$ are the concentrations of free dye initially and at equilibrium, respectively, and I_{dye}^0 and $I_{\text{dye,CB[7]}}^{\infty}$ are the fluorescence intensities of the dye in the absence of

Table 1. Photophysics of Coumarin 1 Dye in Ethanol, Water and Water with the Host CB[7]

dye/CB[7] molar ratio	solvent	λ_{max}^a (nm)	λ_{max}^f (nm)	Φ_f	τ_f (ns)	τ_r (ps)	k_r (10^8 s^{-1})	k_{nr} (10^8 s^{-1})
1:0	ethanol	373	448	0.54	3.09	90	1.75	1.49
1:0	water	380	468	0.04	0.4	72	1.0	24.0
1:20	water	396	468	0.52	5.1	290	1.02	0.94

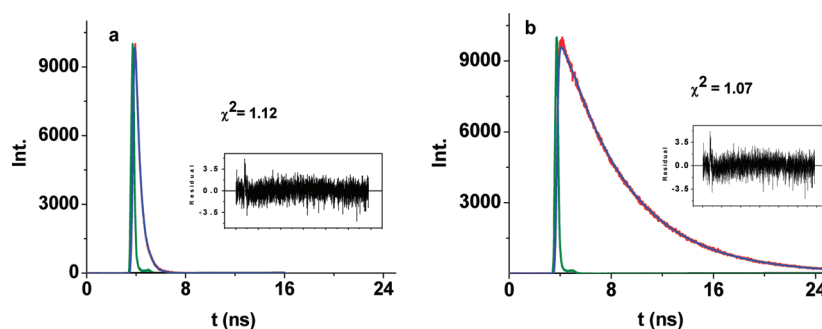


Figure 5. Experimentally measured fluorescence lifetime decays (red lines) of coumarin 1 in (a) water ($\tau_f = 0.4$ ns) and (b) water with a high concentration of CB[7] ($\tau_f = 5.1$ ns; dye/CB[7] = 1:20). Blue lines show fittings, and green lines represent the instrument response function. Inset: Distributions of the weighted residuals for the dye in the corresponding systems.

CB[7] and at a high concentration of CB[7], respectively. The high concentration of CB[7] was selected to obtain all of the dye molecules in complex form. Nonlinear fitting ($\chi^2 \approx 1$) analysis of the increase in fluorescence intensity of the dye as a function of the host concentration yielded an average equilibrium binding constant (K) of $(1.2 \pm 0.1) \times 10^5 \text{ M}^{-1}$ (inset of Figure 4). This value was measured from two independent experiments using different concentrations of the dye. In the fluorescence titration fitting, the increase in the integrated or peak fluorescence intensity (ΔI_f) was used as experimental data, and both approaches gave similar values of K . The formation of a 1:1 dye–CB[7] complex and the K value were also verified by checking the linearity of a double reciprocal plot¹⁹ using the inverse of changes in observed fluorescence intensity $[1/(I_{\text{obs}} - I_f^0)]$ with the inverse of the concentration of the host, $1/[\text{CB}[7]]$.

3.3. Time-Resolved Fluorescence Studies. The dynamic equilibrium features of free dye and dye–CB[7] complex formation were followed by observing the change in fluorescence lifetime (τ_f) of the dye in water upon addition of the host CB[7]. The fluorescence decay of the dye in pure water was found to be monoexponential in nature, corresponding to a lifetime 0.4 ns. Alternatively, the fluorescence decay curve was observed to be monoexponential and fitted to 100% complex dye with a lifetime $\tau_f = 5.1$ ns at a high concentration of the host, that is, at about a 1:20 molar ratio of dye to CB[7] (Figure 5). However, in the presence of lower concentrations of CB[7], the dye lifetime decay curves were biexponential, consisting of two species, free dye and dye complex. Thus, for a 1:1 molar ratio of the dye to the host CB[7], the lifetime decay curve was fitted to two components, 19.4% free dye ($\tau_f = 0.4$ ns) and 80.6% dye–CB[7] complex ($\tau_f = 5.1$ ns). Similarly, upon further addition of CB[7] to the dye solution at a molar ratio of dye/CB[7] = 1:5, the decay curve (Table 2) was fitted to 4.2% free dye ($\tau_f = 0.4$ ns) and 95.8% dye complex ($\tau_f = 5.1$ ns). The increase in the fluorescence lifetime (τ_f) of aqueous solutions of the dye from 0.4 to 5.1 ns upon formation of a complex with CB[7] points toward restricted rotational/vibrational motions of the dye molecule. Free rotational/vibrational motions of the 7-diethylamine moiety in the excited electronic state of the dye were suggested^{13a,15c,20} to dissipate the excitation energy through nonradiative decay rate, which could decrease upon interaction with the cavity of CB[7]. This possibility is supported by values (Table 1) calculated for the radiative (k_r) and nonradiative (k_{nr}) rate constants showing a large decrease in k_{nr} , rather than an increase in k_r , for the dye upon complex formation with CB[7].

Table 2. Analysis of Fluorescence Lifetime Decays and Compositions of Free Dye and Dye Complex in Water at Different Equivalent Ratios of the Host CB[7]

dye/CB[7] molar ratio	τ_f (ns)	τ_f percentage
1:1	0.4 ^a	19.35 ^a
	5.16 ^b	80.65 ^b
1:2	0.4 ^a	15.2 ^a
	5.2 ^b	84.8 ^b
1:5	0.4 ^a	4.2 ^a
	5.16 ^b	95.8 ^b
1:10	0.4 ^a	1.9 ^a
	5.178 ^b	98.1 ^b
1:15	0.4 ^a	0.99 ^a
	5.13 ^b	99.01 ^b
1:20	5.10 ^b	100 ^b

^aFree dye. ^bDye complex.

3.4. Fluorescence Anisotropy Studies. To obtain further insight into the nature of the rotational dynamics of the dye molecule in the absence and presence of the host CB[7], the fluorescence anisotropy was studied. Time-resolved fluorescence anisotropy measurements were carried out in aqueous solutions of the dye in the absence and in the presence of high concentration of the host CB[7] (dye/CB[7] = 1:20). These anisotropy decays were precisely fitted to a single-exponential function, indicating existence of either free or complexed dye. In contrast, observed anisotropy decay curves for the dye at lower CB[7] concentrations support the presence of both species, free and complexed dye.

The measured values of the rotational reorientation time (τ_r) of the dye in water and ethanol were 72 and 90 ps, respectively, which agree with the reported²⁰ values. However, the rotational relaxation of the dye–CB[7] complex in aqueous solution was found to be considerably slower, and thus, the rotational reorientation time was calculated to be much longer in the presence of CB[7]. During the formation of 100% dye complex, upon addition of a high concentration of CB[7], the rotational reorientation time (τ_r) of the dye–CB[7] complex was measured to be 290 ps (Figure 6). The initial anisotropy (r_0) value was estimated to be ~ 0.33 for the dye–CB[7] complex. Thus, evaluation of an increased rotational reorientation time of coumarin 1 dye in water from 72 to 290 ps upon addition of the host CB[7] supports the formation of a strong association complex of the dye with the host (Table 1).

3.5. Rotational Dynamics of the Dye Complex. The evolution of the rotational relaxation dynamics of the fluorescent dye and its complex with the host CB[7] in

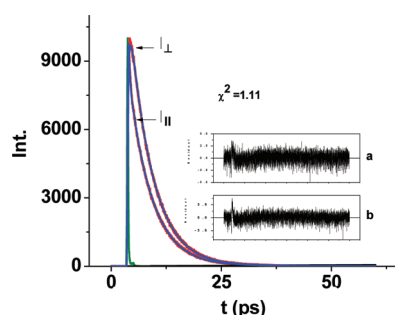


Figure 6. Time-resolved anisotropy decays (maximum count of 10000 for both I_{\parallel} and I_{\perp}) of aqueous solutions of coumarin 1 dye ($\sim 20 \mu\text{M}$) with CB[7] ($\sim 400 \mu\text{M}$) at 25°C . The experimentally measured $I_{\parallel}(t)$ and $I_{\perp}(t)$ functions shown in red and the blue line passing through them are the fits following a single-exponential function, $\tau_r = 290 \text{ ps}$, $\chi^2 = 1.11$. Insets: Distributions of the weighted residuals for (a) $I_{\parallel}(t)$ and (b) $I_{\perp}(t)$.

aqueous solutions can be understood by calculating the frictional forces experienced by the supramolecular entity, in concurrence with experimentally measured rotational reorientation times (section 3.4). According to Stokes–Einstein–Debye (SED) hydrodynamic theory, molecular reorientation is a diffusive process, and the dye rotational reorientation time (τ_r) can be expressed as a function of the hydrodynamic volume (V) of the probe dye molecule and macroscopic solvent characteristics, namely, temperature (T) and viscosity (η). For a spherical probe molecule, the expression is

$$\tau_r = V\eta/k_B T \quad (3)$$

where k_B is the Boltzmann constant. Equation 3 can be modified to account for an axisymmetrical ellipsoidal probe and also for different types of solute–solvent interactions, yielding²⁰

$$\tau_r = (V\eta/k_B T)f(\rho)C(\rho) + \tau_r^0 \quad (4)$$

where $f(\rho)$ is the shape factor of the ellipsoidal probe; $C(\rho)$ describes the solute–solvent friction and has a value that depends on the boundary conditions of the probe and solvent system; and τ_r^0 , a very small term, is identified with free rotation of the probe molecule in a solvent of negligible viscosity. The ellipsoidal shape is defined by the ratio, ρ , of the longitudinal radius to the average equatorial radius, and accordingly, f values can be calculated.²¹ Depending on the probe–solvent friction, the boundary conditions can be either of “stick” or “slip” type. Stick-type hydrodynamic conditions were applicable in this case

because the size of the probe was much larger than that of the solvent molecules.

The coumarin 1 molecule was considered as being close to an oblate ellipsoid. To evaluate the shape factor, $f(\rho)$, and the friction coefficient, $C(\rho)$, for the dye probe, a good estimation of ρ , the ratio of the shorter and longer semiaxes, was needed. Optimization of the ground-state geometry of the coumarin 1 molecule was carried out recently by Gustavsson et al.,²⁰ and their reported dimensions were considered for calculation of τ_r . The three radii of the molecule were reported as 6.35, 4.55, and 1.9 Å. Thus, the hydrodynamic volume of the molecule was calculated to be $V = 23 \times 10^{-29} \text{ m}^3$. For the shorter radius, we considered the value 1.9 Å, but for the longer radius, we used the average of the two values (6.35 and 4.55 Å), or 5.45 Å. Thus, the value of ρ was calculated as $1.9/5.45 = 0.35$. For an oblate ellipsoid with $\rho = 0.35$, we found²¹ the two f values 1.42 and 1.63 for the symmetry axis and the in-plane axis, respectively. The average of these two f values is $\bar{f}(\rho) = 1.52$. Considering stick hydrodynamic boundary conditions and the values of $C(\rho) = 1.0$, $\tau_r^0 = 0$, and $\eta = 0.8903 \times 10^{-3} \text{ Pa s}$ in water, the τ_r value of coumarin 1 was calculated by eq 4 to be 75.7 ps. This calculated value of τ_r is in good agreement with our experimentally measured value (72 ps) for the dye in pure water. Similarly, the τ_r value of the dye in ethanol, which has a higher viscosity ($1.04 \times 10^{-3} \text{ Pa s}$) than water, was calculated to be 88.4 ps, close to the experimentally measured value of 90 ps.

The accuracy of the estimation of the τ_r value of the dye–CB[7] complex depends on the accuracy of the evaluation of its hydrodynamic volume (V). The calculated structure of the CB[7] (see section 3.6) molecule is quite symmetric, having an outer cavity diameter of $\sim 16 \text{ Å}$ and a height of $\sim 9 \text{ Å}$, which agrees closely with the reported^{1d} values. The cavity diameter of the dye–CB[7] inclusion complex was estimated by a quantum chemical calculation based on the circle formed by seven oxygen atoms at one end of the host, which gave a radius of the complex of $r \approx 7.3 \text{ Å}$. The volume of this inclusion complex of CB[7] was also calculated considering the volume inside a contour of 0.001 electrons/Bohr³ density, which gave a volume of $V = 1630 \times 10^{-30} \text{ m}^3$, assuming the complex was close to spheroidal. Thus, the rotational reorientation time (τ_r) of the coumarin 1–CB[7] complex was calculated to be $\sim 353 \text{ ps}$ (using eq 3), slightly longer (by $\sim 18\%$) than our experimentally measured value of $\tau_r = 290 \text{ ps}$ (Table 1). Note that the hydrogen-bonding interactions of the outer cavity of the CB[7] molecule with bulk water molecules could provide an additional frictional force to the complex that was not taken into account for this calculation of τ_r . This would reduce the

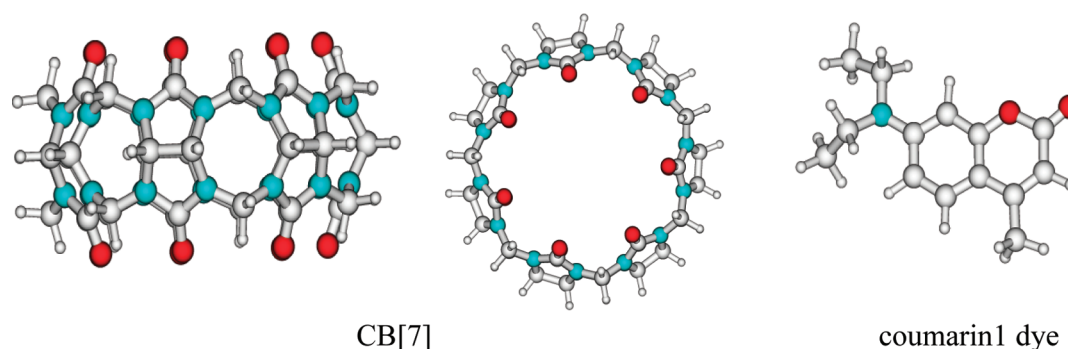


Figure 7. Optimized ground-state structures of coumarin 1 dye and CB[7] host (in two views) calculated at the B3LYP/6-31G(d) level of theory. Color code: red, oxygen; blue, nitrogen; and gray, carbon (large) and hydrogen (small).

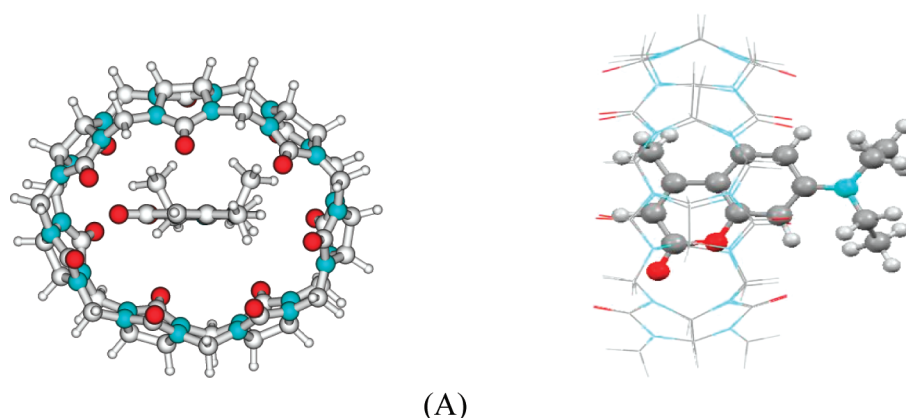


Figure 8. Optimized ground-state structure of the host–guest complex (A) of coumarin 1 dye with CB[7] calculated at the B3LYP/6-31G(d) level of theory. Color code: red, oxygen; blue, nitrogen; and gray, carbon (large) and hydrogen (small). The binding energy of this complex was calculated to be -9.9 kcal/mol.

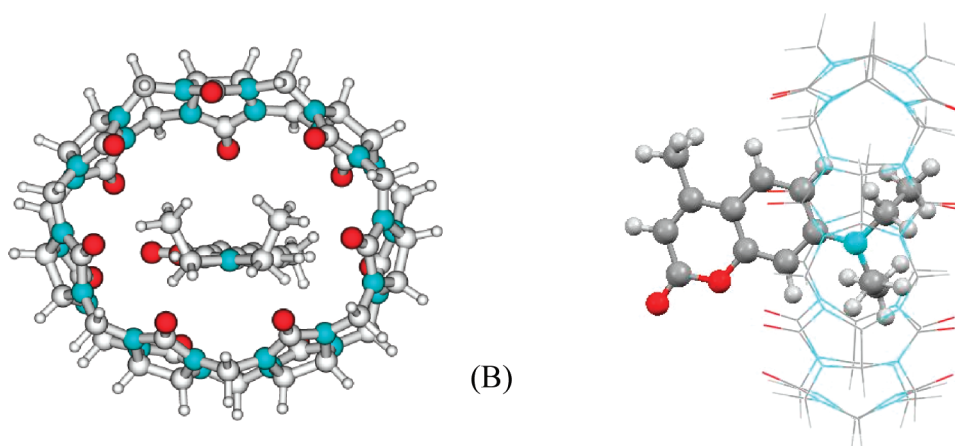


Figure 9. Optimized ground-state structure of the host–guest complex (B) of the dye with CB[7] calculated at the B3LYP/6-31G(d) level of theory. Color code: red, oxygen; blue, nitrogen; and gray, carbon (large) and hydrogen (small). The binding energy of this complex was calculated to be -3.1 kcal/mol.

difference between the calculated and experimentally measured τ_r values of the complex. Hence, a close agreement between the experimentally measured value of τ_r and the calculated value for the dye–CB[7] complex, while considering the inclusion of the coumarin 1 dye molecule inside the CB[7] cavity, confirms the tighter binding and rotation of the whole dye–CB[7] complex as a single entity.

3.6. Structure and Stability of the Host–Guest Complex. The minimum-energy ground-state molecular structures of the coumarin 1 and CB[7] molecules were determined at the B3LYP/6-31G(d) level of theory (Figure 7). Calculation of the CB[7] cavity gave its outer diameter as ~ 16 Å and its height as ~ 9 Å. The length and width of the coumarin 1 dye molecule were calculated as ~ 12 and ~ 9 Å, respectively. This suggests that the dye molecule can enter the host cavity from any one of the longitudinal ends. Different initial structures were considered keeping two different ends of the guest molecule inside the cavity of the host to locate the minimum-energy structure of the host–guest complex. There were 1633 symmetry-adapted basis functions of the inclusion complex including the coumarin 1 dye molecule. A quasi-Newton–Raphson-based algorithm was applied to carry out geometry optimization for each of these systems with various possible conformers as the initial structures. All electronic structure calculations were carried out applying the GAMESS

suite of ab initio programs on a LINUX cluster.²² Finally, two different minimum-energy structures (A and B) were predicted for the complex of coumarin 1 dye with the host CB[7]. In both cases, a good part of the dye molecule remained outside the CB[7] cavity. The binding energy of host–guest complex A (Figure 8 with two different views) was calculated as -9.9 kcal/mol, compared to that of complex B (Figure 9) as -3.1 kcal/mol at the present level of theory. This suggests that the dye molecule prefers to enter the host cavity from its lactone end (complex A) rather than from the 7-diethylamine moiety (complex B). Calculations of various components of the total interaction energy of the host–guest complex were carried out using Kitauro–Morokuma energy decomposition analysis.²³ Energy decomposition analysis performed at the HF level of theory for dye–CB[7] complex A revealed that the electrostatic interaction energy component provided substantially higher stability to the neutral dye (-15.36 kcal/mol). Other interaction components with lower energies, namely, polarization and charge-transfer energies, also provided more stability to the complex of the dye (Table 3). However, an important instability component in the formation of the host–guest complex, namely, the exchange repulsion energy, was found to be $+18.89$ kcal/mol. Note that we did not succeed in performing the same energy decomposition analysis at the DFT level of theory because of convergence problems.

Table 3. Decomposition Analysis of the Interaction Energy of Coumarin 1 Dye–CB[7] Complex at the HF/6-31G(d) Level of Theory

interaction component	dye-CB[7] complex (kcal/mol)
electrostatic energy (ES)	−15.36
exchange repulsion energy (EX)	18.89
polarization energy (PL)	−2.67
	−2.26
	−0.78
total	−5.71
charge-transfer energy (CT)	−3.63
	−5.82
total	−9.45
high-order coupling energy (MIX)	−0.05
total interaction energy	−11.68

The computed minimum-energy structure of complex **A** (Figure 8) indicates that the nitrogen atom of the 7-diethylamino group remains at a close proximity to the CB[7] portal (about 2 Å). The polarity of water in the microenvironment of the hydrophobic CB[7] is expected to be lower than that of the bulk water. Thus, free torsional motion of the amino group is expected to be hindered in aqueous dye–CB[7] complex, destabilizing the formation of the TICT state responsible for the high nonradiative decay rate of the dye. This was validated by observation of a large increase in the fluorescence decay time (τ_f) and yield (Φ_f) of the dye–CB[7] complex in water (see Table 1).

4. CONCLUSIONS

The essentially nonfluorescent ($\Phi_f \approx 0.04$) coumarin 1 dye was converted into a highly fluorescent ($\Phi_f \approx 0.52$) entity in aqueous media by its inclusion within the cavity of the supramolecular host cucurbit[7]uril (CB[7]). A large enhancement in the fluorescence intensity (~ 13 -fold) of the dye in water was observed upon addition of CB[7] in a 1:20 molar ratio. The photophysics, minimum-energy geometry, and interaction energy of the host–guest inclusion complex were investigated in detail by various spectroscopy techniques and DFT-based quantum chemical calculations. The interaction of the dye and CB[7] was stabilized mainly by electrostatic, polarization, and charge-transfer energy components, overcoming the exchange repulsion energy factor and yielding an average equilibrium binding constant K for the dye of $1.2 \times 10^5 \text{ M}^{-1}$. This highly fluorescent complex of coumarin 1 dye would enable the investigation of its applications as probes for biological cells and as active media for developing highly photostable aqueous UV dye lasers.

■ ASSOCIATED CONTENT

Supporting Information

Additional figures, tables, and explanations of spectroscopic techniques for characterizing the guest–host complex and determining its binding constant. This material is available free of charge via the Internet at <http://pubs.acs.org>.

■ AUTHOR INFORMATION

Corresponding Author

*E-mail: alokray@barc.gov.in (A.K.R.), dkmaity@barc.gov.in (D.K.M.).

Notes

The authors declare no competing financial interest.

■ ACKNOWLEDGMENTS

The authors are grateful to Drs. A. K. Das and K. Dasgupta, Laser & Plasma Technology Division; Dr. S. Chattopadhyaya, Bio-Organic Division; Dr. S. K. Ghosh, Theoretical Chemistry Section; and Dr. B. N. Jagtap, Atomic & Molecular Physics Division, of the Bhabha Atomic Research Centre for their support and allowing divisional facilities for this work. M.G. acknowledges the Homi Bhabha National Institute for the award of research fellowship. Sincere thanks are due to the computer centre of BARC for providing the ANUPAM computing facility.

■ REFERENCES

- (1) (a) Johnson, E. R.; Keinan, S.; Sanchez, P. M.; Garcia, J. C.; Cohen, A. J.; Yang, W. *J. Am. Chem. Soc.* **2010**, *132*, 6498–6506. (b) Fenniri, H.; Mathivanan, P.; Vidale, K. L.; Sherman, D. M.; Hallenga, K.; Wood, K. V.; Stowell, J. G. *J. Am. Chem. Soc.* **2001**, *123*, 3854–3855. (c) Kruse, P.; Johnson, E. R.; DiLabio, G. A.; Wolkow, R. A. *Nano Lett.* **2002**, *2*, 807–810. (d) Lagona, J.; Mukhopadhyay, P.; Chakrabarti, S.; Isaacs, L. *Angew. Chem., Int. Ed.* **2005**, *44*, 4844–4870.
- (2) (a) Dooley, C. T.; Dore, T. M.; Hanson, G. T.; Jackson, W. C.; Remington, S. J.; Tsien, R. Y. *J. Biol. Chem.* **2004**, *279*, 22284–22293. (b) Aslan, K.; Gryczynski, I.; Malicka, J.; Matveeva, E.; Lakowicz, J. R.; Geddes, C. D. *Curr. Opin. Biotechnol.* **2005**, *16*, 55–62. (c) Huang, W. H.; Zavalij, P. Y.; Isaacs, L. *Angew. Chem., Int. Ed.* **2007**, *46*, 7425–7427.
- (3) (a) Sheiko, S. S.; Sun, F. C.; Randall, A.; Shirvanyants, D.; Rubinstein, M.; Lee, H.; Matyjaszewski, K. *Nature* **2006**, *440*, 191–194. (b) Yoshizawa, M.; Klosterman, J. K.; Fujita, M. *Angew. Chem., Int. Ed.* **2009**, *48*, 3418–3438. (c) Pattabiraman, M.; Natrajan, A.; Kaliappan, R.; Mague, J. T.; Ramamurthy, V. *Chem. Commun.* **2005**, 4542–4544. (d) DiLabio, G. A.; Piva, P. G.; Kruse, P.; Wolkow, R. A. *J. Am. Chem. Soc.* **2004**, *126*, 16048–16050.
- (4) (a) Croma, A.; Gracia, H.; Navajas, P. M.; Primo, A.; Calvino, J. J.; Trasobares, S. *Chem.–Eur. J.* **2007**, *13*, 6359–6364. (b) Yan, P.; Holman, M. W.; Robustelli, P.; Chowdhury, A.; Ishak, F. I.; Adams, D. M. *J. Phys. Chem. B* **2005**, *109*, 130–137. (c) Sindelar, V.; Silvi, S.; Parker, S. A.; Sobransingh, D.; Kaifer, A. E. *Adv. Funct. Mater.* **2007**, *17*, 694–701. (d) Fabbri, L.; Poggi, A. *Chem. Soc. Rev.* **1995**, *24*, 197–202. (e) Wang, R.; Yuan, L.; Macartney, D. H. *Chem. Commun.* **2005**, 5867–5869.
- (5) (a) Hedges, A. R. *Chem. Rev.* **1998**, *98*, 2035–2044. (b) Uekama, K.; Hirayama, F.; Irie, T. *Chem. Rev.* **1998**, *98*, 2045–2076.
- (6) (a) Jiao, D.; Zhao, N.; Scherman, O. A. *Chem. Commun.* **2010**, 46, 2007–2009. (b) Kim, J.; Jung, I.-S.; Kim, S.-Y.; Lee, E.; Kang, J.-K.; Sakamoto, S.; Yamaguchi, K.; Kim, K. *J. Am. Chem. Soc.* **2000**, *122*, 540–541. (c) Day, A.; Arnold, A. P.; Blanch, R. J.; Snushall, B. *J. Org. Chem.* **2001**, *66*, 8094–8100.
- (7) (a) Hennig, A.; Bakirci, H.; Nau, W. *Nat. Methods* **2007**, *4*, 629–632. (b) Mohanty, J.; Bhasikuttan, A. C.; Nau, W. M.; Pal, H. *J. Phys. Chem. B* **2006**, *110*, 5132–5138. (c) Soufi, W. A.; Reija, B.; Felekyan, S.; Seidel, C. A. M.; Novo, M. *ChemPhysChem* **2008**, *9*, 1819–1827. (d) Gadde, S.; Batchelor, E.; Weiss, J. P.; Ling, Y.; Kaifer, A. E. *J. Am. Chem. Soc.* **2008**, *130*, 17114–17119.
- (8) (a) Halterman, R. L.; Moore, J. L.; Yakshe, K. A.; Halterman, J. A. I.; Woodson, K. A. *J. Incl. Phenom. Macrocycl. Chem.* **2010**, *66*, 231–241. (b) Arunkumar, E.; Forbes, C. C.; Smith, B. D. *Eur. J. Org. Chem.* **2005**, 4051–4059.
- (9) Navajas, P. M.; Corma, A.; Garcia, H. *ChemPhysChem* **2008**, *9*, 713–720.
- (10) Mohanty, J.; Nau, W. M. *Angew. Chem., Int. Ed.* **2005**, *44*, 3750–3754.
- (11) (a) Mohanty, J.; Pal, H.; Ray, A. K.; Kumar, S.; Nau, W. M. *ChemPhysChem* **2007**, *8*, 54–56. (b) Mohanty, J.; Jagtap, K.; Ray, A. K.; Nau, W. M.; Pal, H. *ChemPhysChem* **2010**, *11*, 3333–3338.
- (12) (a) Wyman, I. W.; Macartney, D. H. *Org. Biomol. Chem.* **2010**, *8*, 247–252. (b) Hettiarachchi, G.; Nguyen, D.; Wu, J.; Lucas, D.; Ma,

- D.; Isaacs, L.; Briken, V. *PLoS One* **2010**, *5*, e10514. (c) Uzunova, V. D.; Cullinane, C.; Brix, K.; Nau, W. M.; Day, A. I. *Org. Biomol. Chem.* **2010**, *8*, 2037–2042. (d) Nau, W. M. *Nature Chem.* **2010**, *2*, 248–250.
- (13) (a) Wagner, B. D. *Molecules* **2009**, *14*, 210–237. (b) Seth, D.; Chakroborty, A.; Setua, P.; Sarkar, N. *Langmuir* **2006**, *22*, 7768–7775. (c) Guan, H.; Zhu, L.; Zhou, H.; Tang, H. *Anal. Chim. Acta* **2008**, *608*, 73–78. (d) Kuznetsova, N. A.; Kalia, O. L. *Russ. Chem. Rev.* **1992**, *7*, 683–696.
- (14) (a) Wang, R.; Bardelang, D.; Waite, M.; Udachin, K. A.; Leek, D. M.; Yu, K.; Ratcliffe, C. I.; Ripmeester, J. A. *Org. Biomol. Chem.* **2009**, *7*, 2435–2439. (b) Barooah, N.; Pemberton, B. C.; Sivaguru, J. *Org. Lett.* **2008**, *10*, 3339–3342. (c) Nau, W. M.; Mohanty, J. *Int. J. Photoenergy* **2005**, *7*, 133–141.
- (15) (a) Kubin, R. F.; Fletcher, A. N. *Chem. Phys. Lett.* **1983**, *99*, 49–52. (b) Jones, G., II; Jackson, W. R.; Choi, C. Y.; Bergmark, W. R. *J. Phys. Chem.* **1985**, *89*, 294–300. (c) Brackmann, U. *Lambdachrome Laser Dyes*; Lambda Physik GmbH: Göttingen, Germany, 1986; pp III-66–III-67. (d) Arbeloa, T. L.; Arbeloa, F. L.; Tapia, M. J.; Arbeloa, I. L. *J. Phys. Chem.* **1993**, *97*, 4704–4707.
- (16) Moog, R. S.; Kim, D. D.; Oberle, J. J.; Ostrowski, S. G. *J. Phys. Chem. A* **2004**, *108*, 9294–9301.
- (17) Nau, W. M.; Florea, M.; Assaf, K. I. *Isr. J. Chem.* **2011**, *51*, 559–577.
- (18) Mohanty, J.; Bhasikuttan, A. C.; Nau, W. M.; Pal, H. *J. Phys. Chem. B* **2006**, *110*, 5132–5138.
- (19) Singh, M. K.; Pal, H.; Koti, A. S. R.; Sapre, A. V. *J. Phys. Chem. A* **2004**, *108*, 1465–1474.
- (20) Gustavsson, T.; Cassara, L.; Marguet, S.; Gurzadyan, G.; van der Meulen, P.; Pommeret, S.; Mialocq, J.-C. *Photochem. Photobiol. Sci.* **2003**, *2*, 329–341.
- (21) Flemming, G. R. *Chemical Applications of Ultrafast Spectroscopy*; Oxford University Press: New York, 1986; p 132.
- (22) Schmidt, M. W.; Baldrige, K. K.; Boatz, J. A.; Elbert, S. T.; Gordon, M. S.; Jensen, J. H.; Koseki, S.; Matsunaga, N.; Nguyen, K. A.; Su, S. J.; Windus, T. L.; Dupuis, M.; Montgomery, J. A. *J. Comput. Chem.* **1993**, *14*, 1347–1363.
- (23) Chen, W.; Gordon, M. S. *J. Phys. Chem.* **1996**, *100*, 14316–14328.